UNCLASSIFIED

Defense Technical Information Center Compilation Part Notice

ADP011168

TITLE: Developments of Adaptive Methods for Active Instability Control

DISTRIBUTION: Approved for public release, distribution unlimited

This paper is part of the following report:

TITLE: Active Control Technology for Enhanced Performance Operational Capabilities of Military Aircraft, Land Vehicles and Sea Vehicles [Technologies des systemes a commandes actives pour l'amelioration des performances operationnelles des aeronefs militaires, des vehicules terrestres et des vehicules maritimes]

To order the complete compilation report, use: ADA395700

The component part is provided here to allow users access to individually authored sections of proceedings, annals, symposia, etc. However, the component should be considered within the context of the overall compilation report and not as a stand-alone technical report.

The following component part numbers comprise the compilation report:
ADP011101 thru ADP011178

UNCLASSIFIED

Developments of Adaptive Methods for Active Instability Control

M. Mettenleiter and S. Candel

Laboratoire E.M2.C, CNRS, Ecole Centrale Paris, F-92295 Châtenay-Malabry Cedex

Abstract

Adaptive algorithms are considered in many applications of active flow control. Independent on the controller type, it is always necessary to provide information on the system to be controlled. A standard method is to identify the system in a first step and then provide the result to the controller. The secondary path information obtained is necessary for the proper convergence of the adaptive filter. This two-step procedure is applicable in many cases but it is not sufficient when the system changes significantly during operation.

This study focuses on self adaptive controllers operating with an on-line identification procedure. These systems are devised in this article to control aeroacoustic instabilities of the type found in segmented solid rocket motors. Instabilities are driven by vortex shedding which are coupled by a resonant mode of the system. Two laboratory scale experiments are used as testbeds for the control schemes. Self adaptive control is compared with a standard adaptive method using an off-line identification procedure.

1 Introduction

Research on active control has taken considerable momentum with a rapid expansion of domains of application. Many developments have concerned control of flow instabilities. External and internal aerodynamics have been considered, the special case of combustion has received much attention (see McManus et al. [1] for a review of the control of combustion instabilities). These instabilities are observed in many practical systems (jet engines, rocket motors, gas turbines, ...) and they have many undesirable effects.

Active means of their reduction or suppression have been devised in recent years. Control methods in this area are mainly based on feedback principles in which the signal detected by a sensor is returned through the controller unit to an actuator which injects perturbations into the combustor. Initial developments were based on simple control concepts, the sensor signal was just amplified and phase delayed and then returned to the actuator. Instabilities were reduced quite successfully but it was soon found that the method was only applicable in a limited range of operation of the combustor. An important progress was made by replacing the gain and phase control by adaptive algorithms (Billoud et al. [2]). It was shown that control could be achieved over an extended domain around the nominal point of operation. The adaptive controller was able to follow the changes in the mode of combustion and different types of instabilities were reduced leading to a significant augmentation of the stability domain of the combustor. Adaptive techniques have been applied in many other areas with notable developments in anti-sound and active vibration control (see the books of Nelson and Elliott [3], Kuo and Morgan [4] and articles by Eriksson [5], [5], [6], [7] and Kuo and Morgan [8]). Methods of adaptive filtering and adaptive control are well described by Widrow and Stearns [9], Haykin [10], Goodwin and Sin [11] or by Åström and Wittenmark [12] amongst others. Glentis et al. [13] give a general introduction to LMS (least mean square methods) which have been extensively used in recent years.

Whatever the structure of the control algorithm is, it is always necessary to have some information on the system to be controlled. The adaptive methods explored up to now in experimental combustion and flow control applications have relied on information obtained from an off-line identification process. The so called "secondary path" which corresponds to the system as it is seen by the controller is described by a transfer function $\hat{S}$ (filter) which is identified in a first step. When the secondary path is essentially acoustic (ie featuring a microphone as sensor and a driver unit as actuator) the transfer function does not change too much with the operating conditions and the result of identification may be used over a certain range of

Paper presented at the RTO AVT Symposium on "Active Control Technology for Enhanced Performance Operational Capabilities of Military Aircraft, Land Vehicles and Sea Vehicles", held in Braunschweig, Germany, 8-11 May 2000, and published in RTO MP-051.

operating conditions. If however the secondary path involves a convective process, the identification will be valid in a very limited range of flow parameters.

If the secondary path $\boldsymbol{S}$ differs markedly from its representation in the control algorithm $\hat{\boldsymbol{S}}$, the adaptive filter $\boldsymbol{W}$, which amplifies and dephases the sensor signal to produce the controller output, will not converge. One may show that the problem arises when the error in phase of $\hat{\boldsymbol{S}}$ with respect to that of $\boldsymbol{S}$ exceeds $\pm 90°$. When the difference between the real and identified systems is too important it is necessary to update the model in order to maintain control. This could be accomplished by incorporating the identification procedure in the controller. The combination of identification and control is now seen as a key issue in the development of practical controllers.

In the active control of aeroacoustic vortex instabilities of solid rocket motors, which motivates the present study, on–line identification is the only possible strategy for practical implementation. It is presumed that a model for the secondary path with fixed parameters will not be able to render the changes taking place during operation of the motor. Even if some information is available on the system, it may only be used as a starting description with the on-line identification progressively taking-over during the control process.

Self adaptive control (SAC) or equivalently adaptive control with on-line identification are explored in the domain of anti-sound and vibration control and some experimental investigations are available. Theoretical studies of the application of SAC to combustion instabilities are also reported (see for example Koshigoe et al. [14]). The system is described by a reduced order dynamical model which provides a simplified representation of the real behavior. The practical implementation of SAC in flow instability experiments is not found in the technical literature.

The objective of this article is to describe some of our results on self adaptive control. This topic has been systematically investigated in order to control aeroacoustic instabilities. A comparison between the different possible structures of controllers incorporating on-line identification was carried out using an experimental testbed "CAPS". Performance of SAC was measured with respect to that of adaptive control with off-line identification. Self adaptive control was also achieved in a model scale experiment representing the geometry of a segmented solid rocket motor (detailed results are reported in [15]).

We begin with a description of self adaptive control concepts (section 2). The self adaptive controller structure is discussed in section 3. Selected test results are given in section 4 and 5 for two different experiments.

2 Self adaptive control concepts

Most of the self adaptive algorithms used in the area of instability control are inspired by schemes developed in the anti–noise domain. These algorithms normally operate with at least two sensors. The primary sensor signal x is used as input of the controller and the secondary or error sensor signal e provides a measure for quantifying the success of control (refer to Figures 1 or 2). Using x (which is generally stationary or slowly varying) as signal which is correlated to the primary noise d, the objective is to generate an anti–noise signal y_r to counteract d. If the error sensor signal e is reduced, the control is successful. As can be seen in the two figures, an estimate $\hat{\boldsymbol{S}}$ of the secondary path is necessary in order to properly adapt the filter coefficients of $\boldsymbol{W}$.

In configurations using off–line identification, this transfer function can be determined by using for example a white noise signal to excite $\boldsymbol{S}$. The filter $\hat{\boldsymbol{S}}$ is then determined as to match as close as possible the output of $\boldsymbol{S}$.

In schemes using on–line identification of the secondary path, two basic structures can be distinguished. The first uses an additional signal (white noise for example) for identifying the secondary path (an example from Kuo and Morgan [4] is shown in Figure 1). The second structure is using the filter output of $\boldsymbol{W}$, the signal y, as input of the secondary path estimation $\hat{\boldsymbol{S}}$ (see an example from Kuo and Morgan [4] in Figure 2). Note that in this example the signal y corresponds to the shifted primary sensor signal during a first "identification phase".

The objective of the two structures is to get an estimate of the error signal e by using a system modeling procedure (shown in the lower half of the two figures). As the signal e comprises two components (d and y_r), it is sufficient to use two filters to reproduce an estimate of these signals to form an estimate $\hat{e}$. One of the filters ($\hat{\boldsymbol{S}}$) represents an estimate of the real secondary path. Therefore it can be used to calculate the signal x' for the control algorithm. Control and system modeling (that is identification) is performed at the same time for the scheme in Figure 1. Figure 2 proposes first an identification procedure carried out off–line (in the presence of the instability phenomenon) before switching to the real control with continued identification on–line.

Kuo and Morgan [4] note two important conditions which should be fulfilled by self–adaptive algorithms.

First, the estimation of $\hat{\boldsymbol{S}}$ should be independent of the filter $\boldsymbol{W}$. This guarantees robustness of the algorithm. The structure proposed in Figure 1 fulfills this requirement: the white noise signal helps getting an estimate $\hat{\boldsymbol{S}}$ which is independent of the filter $\boldsymbol{W}$. The second requirement demands that the estimation of $\hat{\boldsymbol{S}}$ should not interfere with control. This is not the case for the scheme proposed in Figure 1 (the white noise signal interferes with y and perturbs the control). The algorithm in Figure 2 does fulfill the second requirement, but not the first. As y is generally narrow band, $\hat{\boldsymbol{S}}$ will not be correctly identified on the whole frequency band of interest. One can see that the two conditions cannot be fulfilled at the same time and hence a compromise has to be found between interference and robustness.

3 Self adaptive structure for control at the noise source

In anti–noise situations it is generally easy to use several sensors. The primary sensor may measure a signal which is correlated with the primary noise generated later on (this signal could for example be the angular rotation of a motor) and the error sensor measures the pressure fluctuations in the passenger cabin for example. If only one sensor is employed, the error signal is used to reconstruct an estimate of the primary noise which replaces x in the Figures shown in the last section. Note, that for this estimate $\hat{d}$ the same assumption holds as for the signal x: it does not change rapidly during operation.

Control schemes for combustion or aeroacoustic instabilities differ from the usual concepts adopted in the area of pure noise control based on anti–noise principles. It has been pointed out that generally the primary sensor signal x (or $\hat{d}$) does not change rapidly in noise control. But this is the case for combustion or aeroacoustic problems. The control acts on the noise source (the unsteady heat release in combustion problems or the regular vortex shedding in aeroacoustic instabilities). Therefore, a different control scheme should be employed in these situations (see Mettenleiter et al. [16] for more details). If only one sensor is used, the controller input x (or $\hat{d}$) is now replaced by the error signal e. This difference can be seen in the upper part of Figure 3. Examining the behaviour during control, one can write :

$$\begin{aligned} e &= d - y_r \\ e &= d - \boldsymbol{SW}e \\ (I + \boldsymbol{SW})e &= d \end{aligned}$$

$$e = \frac{d}{I + \boldsymbol{SW}}.$$

It can be seen that this controller only converges towards a stable state $e \to 0$ if the primary noise d itself is modified and driven to zero. This is contrary to a classical anti–noise situation with $y_r \to d$ for $e \to 0$ (and $d = cnst.$).

The lower part of Figure 3 represents the system modeling. As in the schemes shown in the previous section, the aim of this modeling part is to reproduce the error signal e. This estimate is called $\hat{e}$ and it is composed of two components: $\hat{y}_r$ which reproduces the output of the secondary path and $\hat{d}$, which is an estimate of the primary noise d.

The identification process adopted in this scheme does not interfere with the adaptive control. As indicated above, the method is not without problems:

- The input signal of $\hat{\boldsymbol{S}}$ is not normally wide band and as a consequence identification is only carried out in a narrow band an not in the full range of frequencies

- The filter coefficients may diverge because the solution is not unique (adaption of different filters at the same time causes problems if their input signal is not decorrelated, see for example [9]). Divergence of the coefficients can also be observed in real time applications if the input signal is not persistently exciting the filter (see for example [4]).

The first point is not too critical. It is in fact sufficient to get an secondary path estimation which is sufficiently precise for the frequency range of the instability. If this range changes during operation, the algorithm may adapt itself to the new frequencies.

The second point is more problematic. For successful control long term divergence problems have to be resolved. This can be done in different ways. It is possible to observe the coefficient adaptation history and adjust a leak coefficient. Starting from a solution which satisfies a certain criterion one may augment or reduce the leak coefficient in order to stay close to this criterion. If the estimated filter coefficients do not allow a proper operation of the controller (because the operating point has changed) one defines a new criterion for the filter coefficients.

A second strategy consists in freezing the coefficient adaptation of $\boldsymbol{F}^{11}$ and $\hat{\boldsymbol{S}}$ if the model represented by these two filters features a response which comes close to that of the real system. If the model does not reflect reality, the learning process should be resumed. The adaptation of $\boldsymbol{F}^{11}$ and $\hat{\boldsymbol{S}}$ proceeds until the model represents again the real system with a sufficient precision. One may thus avoid problems of model divergence over a long period of operation.

It is interesting to analyze the system in the steady state. The three error functions in Figure 3 are given by :

$$\begin{aligned} e &= d - \boldsymbol{SW}e \\ e_2 &= (d - \boldsymbol{SW}e) - (\boldsymbol{F}^{11} - \hat{\boldsymbol{S}}\boldsymbol{W})e \\ \hat{e} &= (\boldsymbol{F}^{11} - \hat{\boldsymbol{S}}\boldsymbol{W})e. \end{aligned}$$

The first expression has the same solution as shown above. The third equation gives the estimate of the error sensor simulation. In the second equation, this estimate is compared with the sensor signal in order to adjust the filters $\boldsymbol{F}^{11}$ and $\hat{\boldsymbol{S}}$. One possible solution for minimizing e_2 is given by :

$$\hat{\boldsymbol{S}}^{0} = \boldsymbol{S}.$$

In this case, the filter $\boldsymbol{F}^{11}$ becomes :

$$\boldsymbol{F}^{11^{o}} = \frac{d}{e}$$

and it follows that $\hat{d} = d$. It might be disturbing to represent the primary noise as a function of the error signal $\hat{d} = \boldsymbol{F}^{11}e$. This follows the assumption that the primary noise is proportional to the error signal itself and it holds only if control acts at the source of the noise.

4 Flow instability control in a laboratory testbed

Different SAC algorithms (with and without additional white noise) have been developed and tested on a simple laboratory scale experiment (see Figure 4) designed to reproduce some features of aeroacoustic coupling of the kind observed in solid rocket motors. Air is injected in the lower part of the device. The small cavity acts as a "vortex generator". The number of vortices and their frequency are determined by the eigenmodes of the setup, the position of the cavity with respect to the eigenmodes and the flow speed (see [17] or [16] for more details about the phenomena). Certain volume flows lead to a strong acoustic resonance. The pressure fluctuations can be measured by different microphones. Velocity fluctuations in the cavity are detected by a hot film probe.

We will present in this paper a comparison between one of the SAC algorithms (introduced in Figure 3) and the equivalent scheme with off-line identification of the secondary path (denoted as "reference"). Both controllers work with the same sampling frequency (3 kHz) and contain FIR filters with 64 coefficients for $\boldsymbol{W}$ and 90 tabs for $\hat{\boldsymbol{S}}$. In addition to that, the filter $\boldsymbol{F}^{11}$ for the SAC scheme contains 32 elements. During the tests, the reference algorithm is started with the knowledge of $\hat{\boldsymbol{S}}$, the filter $\boldsymbol{W}$ is initialized with zero and adapts during control. The SAC scheme starts with no knowledge and all three filters adapt at the same time during the first period of control.

The merits of the algorithms may be rated at different levels:

- Comparison of the steady state after convergence
- Rapidity of the transient response
- Comparison of the transfer functions of $\hat{\boldsymbol{S}}$ and $\boldsymbol{W}$ after convergence

In what follows, we compare the two algorithms with respect to the three points noted above. Although only one volume flow rate is shown here, these results are representative for the whole domain of application of the setup.

4.1 Comparison of the steady state after convergence

A volume flow rate of 16 m^3/h is injected into the experimental device. The instability develops and the resulting pressure fluctuations are measured and the spectrum is calculated. Then, the controller is switched on and after convergence a second spectrum is obtained. These spectra are shown in Figure 5 on the left for the reference algorithm and on the right for the SAC scheme. Dashdotted lines represent the spectra without control, the solid lines are obtained with control. A comparison between the two algorithm shows a slightly better performance for the reference controller. The reduction in the main peak is about 40 dB (compared to 35 dB for the SAC). The first harmonic at 1100 Hz is also reduced. An intermediate peak at 800 Hz is slightly increased by both schemes, whereas the increase for the SAC algorithm is more important. Nevertheless, the main frequency is largely reduced and the self–adaptive controller performs equally well.

4.2 Rapidity of the transient response

The speed of convergence is compared for the same volume flow rate as above. The reference algorithm is shown on the left of Figure 6 while the SAC scheme is displayed on the right. The top image shows the error sensor signal, the bottom image visualizes the controller output. The vertical line indicates the switch on of the algorithm.

The reference algorithm shows a quick reduction of the pressure signal. The controller output reaches large amplitudes at the beginning of control. Later on a relatively small component is sufficient to maintain control. This behaviour is typical for algorithms acting at the source of noise: once, the feedback mechanism which leads to instability is broken, only a small amount of energy is necessary to prevent the growth of the phenomenon. The SAC scheme needs more time to react. After a first period where the pressure signal is not noticeably reduced (the controller output as well is small), the reduction takes place and a comparable steady state behaviour is reached (note the different scalings between the figures). This additional delay is attributed to the learning phase of $\hat{\boldsymbol{S}}$ and $\boldsymbol{F}^{11}$ during which the controller does not (and can not) act properly.

4.3 Comparison of $\hat{\boldsymbol{S}}$ and $\boldsymbol{W}$ after convergence

It is particularly interesting to compare the secondary path estimation and the filter $\boldsymbol{W}$ for the two control algorithms. This may show if the SAC scheme converges towards the reference solution or not.

Using the same operating conditions as above, the filter coefficients have been acquired and their transfer functions are calculated. The left of Figure 7 shows the secondary path estimation $\hat{\boldsymbol{S}}$, the right displays the behaviour of the $\boldsymbol{W}$ filter (the amplitude is on the top, the corresponding phase on the bottom of the figures). The reference filters are printed with dashed lines, the SAC filters are shown with solid lines.

The amplitude of the SAC estimation $\hat{\boldsymbol{S}}$ does not correspond well to the path identified off-line. More important than the amplitude is the phase behaviour of $\hat{\boldsymbol{S}}$. Close to the frequency of the instability (550 Hz) the SAC phase is indeed close to the reference phase. Other frequencies (particularly the lower ones) are not contained in the error signal and hence the identification does not work for these components. Using an additional white noise signal for the identification procedure, all frequencies could be excited and a valid estimate could be obtained for the whole range of interest.

The comparison of the $\boldsymbol{W}$ coefficients shows a similar behaviour for the two algorithms. The amplitudes are comparable for the 550 Hz component (although it seems as if the reference algorithm shifts its action closer to 500 Hz). The 820 Hz component, the second frequency appearing in the spectra of Figure 5, is equally amplified by $\boldsymbol{W}$ for the two algorithms. The phases of the two schemes correspond well, particularly for the frequencies of interest. This indicates that the SAC scheme converges toward a solution comparable to the reference algorithm.

5 Control of a model of a segmented solid rocket motor

The experimental setup PLEXI used at the Von Kármán Institute in Belgium for studies concerning aeroacoustic noise generation in segmented solid propellant boosters is a down-scale cold flow facility of the P230 accelerator of the Ariane–5 rocket. The setup is based on a 1/15–scale similarity with the full scale motor obtained by conserving the Mach number when 50 % of the propellant is burnt (see Figure 8). The length of the test section is 1.26 m, the internal diameter is given by 11.3 cm. The inhibitor height is 17.4 mm and the inhibitor–nozzle distance of 14 cm corresponds to an optimized flow acoustic coupling (for more details about the setup, refer to [18] and [19]). Adaptive control was used in order to study the influence of the acoustics on the vortex driven instabilities (the results are shown in Ref. [20]).

The SAC algorithm described before has been tested in this facility and results are again compared to the reference scheme using off–line identification. The performance after convergence of the algorithms is shown in Figure 9. The results for the reference algorithm appear on the left, on the right the SAC scheme is shown. Dashed lines indicate pressure spectra without and solid lines with control. As in the previous example, the reference scheme shows a slightly better behaviour. Note that for this experiment the reference scheme uses a higher sampling frequency and longer filters.

The transient behaviour can be examined in Figure 10. The reference case is on the left, the SAC algorithm is shown on the right. The top plots represent the error signal (pressure sensor), the bottom plots specify the controller output. The vertical line indicates the switch on of the controller. Again, the reference scheme shows a better transient behaviour. The controller output grows faster than for the SAC algorithm. Nevertheless, the steady state is comparable for the two controllers.

Again, the results shown here for the SAC scheme are representative for the behaviour on a larger domain of application. These results are documented in Ref. [15].

6 Conclusion

Self adaptive control schemes are investigated in this article for active control applications. The control of aeroacoustic instabilities driven by large scale vortices is specifically considered. Two experimental facilities serve as testbeds for control. The self adaptive controller is compared with more standard adaptive methods relying on off-line identification procedures. It is shown that the self adaptive controller is able to achieve control. Convergence is slowed down by the additional task of identification. The steady state behaviour is nearly as good as with the reference algorithm and the different filters show similar behaviour for the different algorithms. Long term divergence problems, often encountered in real time implementations, are resolved by monitoring the development of the different filter coefficients.

Acknowledgments: This research was supported in part by CNES and ONERA in the framework of the ASSM project. The authors are also grateful to J. Anthoine from VKI Bruxelles for providing the PLEXI facilities.

References

[1] K. R. McManus, T. Poinsot, and S. Candel. A rieview of active control of combustion instabilities. *Prog. Energy Combust. Sci.*, 19:1–29, 1993.

[2] G. Billoud, M. A. Galland, C. Huynh Huu, and S. Candel. Adaptive active control of combustion instabilities. *Combust. Sci. and Tech.*, 81:257–283, 1992.

[3] P. A. Nelson and S. J. Elliot. *Active Control of Sound.* Academic Press, 1992.

[4] Sen M. Kuo and Dennis R. Morgan. *Active Noise Control Systems.* John Wiley & Sons, 1996.

[5] L.J. Eriksson and M.C. Allie. Use of random noise for on–line transducer modeling in an adaptive active attenuation system. *J. Acoust. Soc. Am.*, 85(2):797–802, 1989.

[6] L. J. Eriksson. Development of the filtered–u algorithm for active noise control. *J. Acoust. Soc. Am.*, 89(1):257–265, 1991.

[7] L.J. Eriksson. Active sound and vibration control: A technology in transition. *Noise Control Eng. J.*, 44(1):1–9, 1996.

[8] S.M. Kuo and D.R. Morgan. Active noise control: A tutorial review. *Proceedings of the IEEE*, 87(6):943–973, 1999.

[9] B. Widrow and S. D. Stearns. *Adaptive Signal Processing.* Prentice Hall, 1985.

[10] S. Haykin. *Adaptive Filter Theory.* Prentice Hall, 1991.

[11] G. C. Goodwin and K.S. Sin. *Adaptive Filtering, Prediction and Control.* Prentice Hall, 1984.

[12] Karl J. Åström and Björn Wittenmark. *Adaptive Control.* Addison-Wesley, 1995.

[13] K. Berberidis G.O. Glentis and S. Theodoridis. Efficient least squares adaptive algorithms for fir transversal filtering. *IEEE Signal Processing Magazine*, July:13–41, 1999.

[14] S. Koshigoe, T. Komatsuzaki, and V. Yang. Active control of combustion instabilities with on–line system identification. In *34th. Aerospace Sciences Meeting & Exhibit, Reno, Jan. 15–18.* AIAA Paper 96-0759, 1996.

[15] M. Mettenleiter. *Contrôle adaptatif des instabilités aéroacoustiques. Application aux systèmes de propulsion.* PhD thesis, Ecole Centrale Paris, 2000.

[16] M. Mettenleiter, E. Haile, and S. Candel. Adaptive control of aeroacoustic instabilities. *J. Sound Vib.* (in press), 2000.

[17] M. Mettenleiter, E. Haile, and S. Candel. Adaptive control of aeroacoustic instabilities with application to propulsion systems. In *RTO Symposium on "Gas Turbine Engine Combustion, Emission and Alternative Fuels", Lisbon, Portugal, 12–16 october*, 1998. RTO–MP–14 AC/323(AVT)TP/10.

[18] P. Planquart J. Anthoine and D. Olivari. Cold flow investigation of the flow acoustic coupling in solid propellant boosters. In 36^{th} *Aerospace Sciences Meeting.* AIAA, 1998. Paper 98-0475.

[19] J. Anthoine and D. Olivari. Cold flow simulation of vortex induced oscillations in a model of solid propellant boosters. AIAA Paper 99–1826, 1999.

[20] J. Anthoine, M. Mettenleiter, O. Repellin, J.-M. Buchlin, and S. Candel. Influence of adaptive control on vortex driven instabilities in a scaled model of solid propellant motors. *J. Fluid Mechanics* (submitted), 2000.

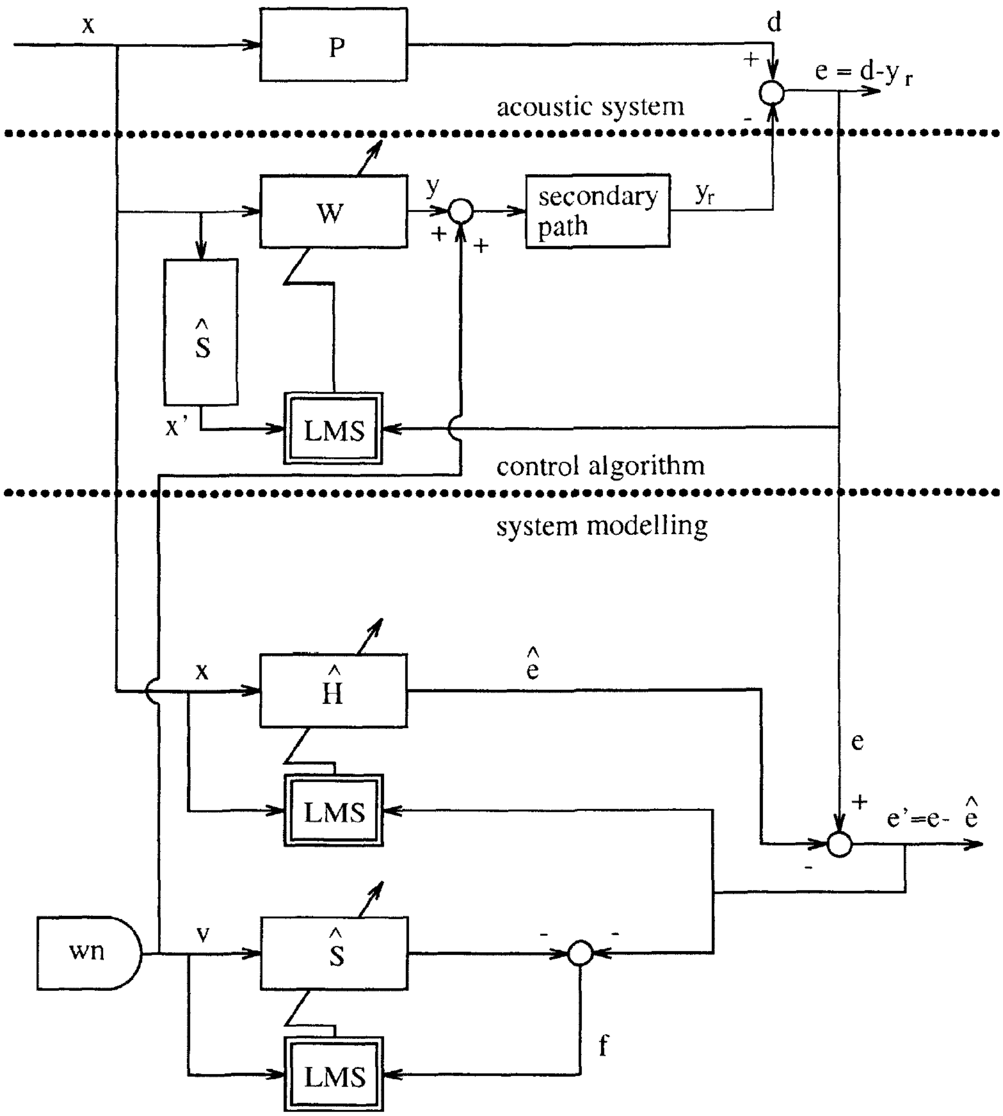

Figure 1: Self-adaptive anti-noise algorithm using a white noise signal for the identification procedure and two sensors.

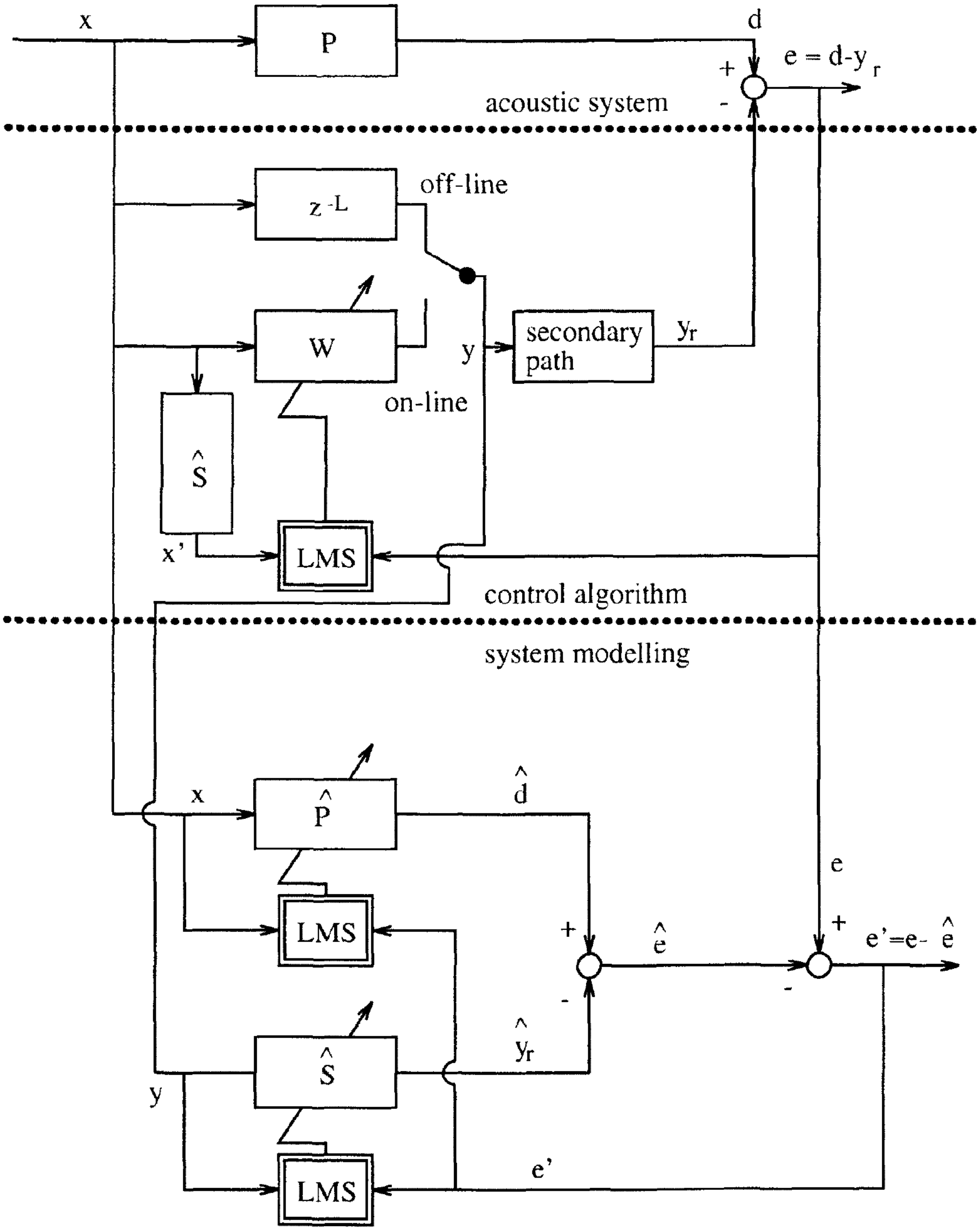

Figure 2: Self-adaptive overal modelling anti-noise algorithm using two sensors.

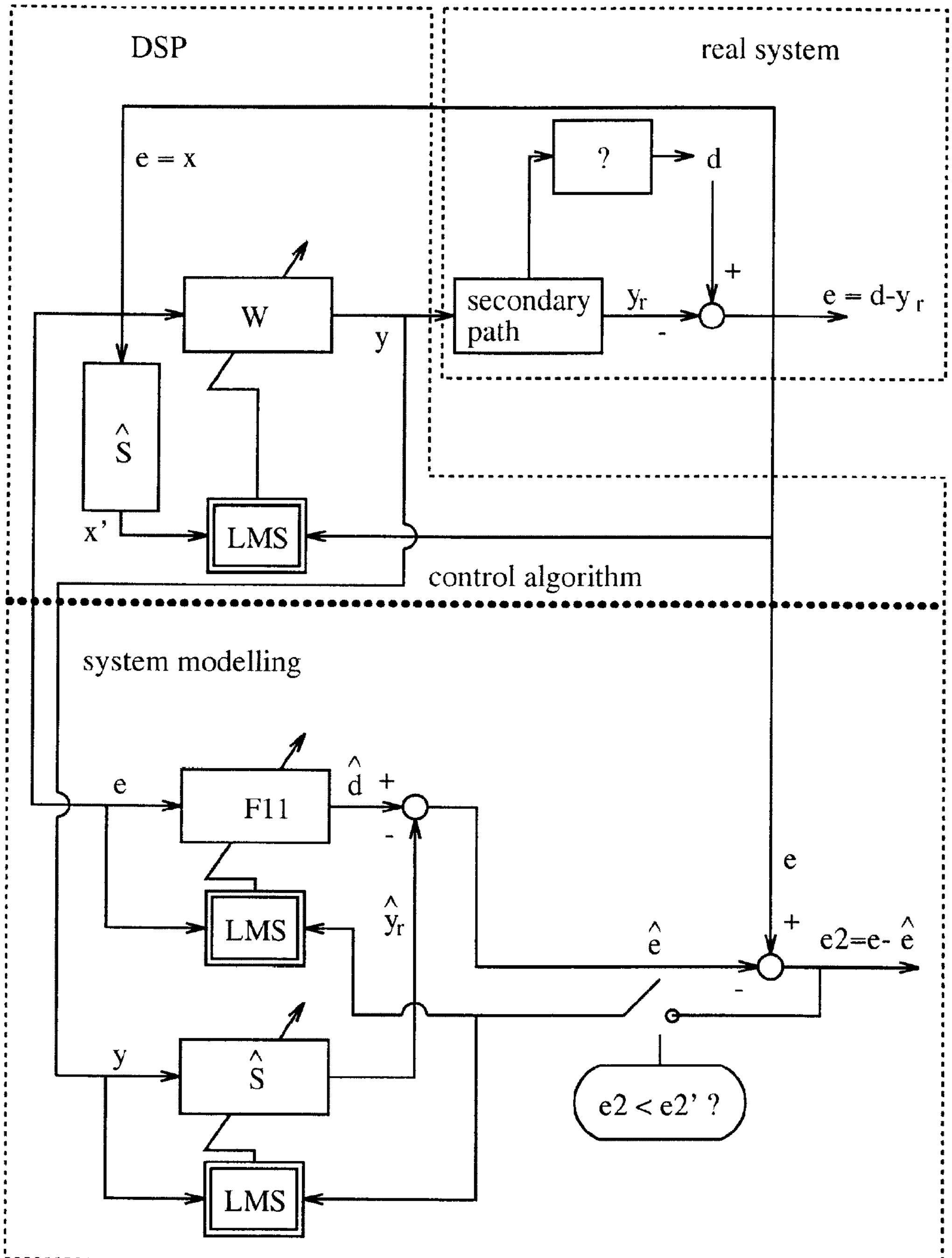

Figure 3: Self-adaptive overall modelling noise source control algorithm using one sensor.

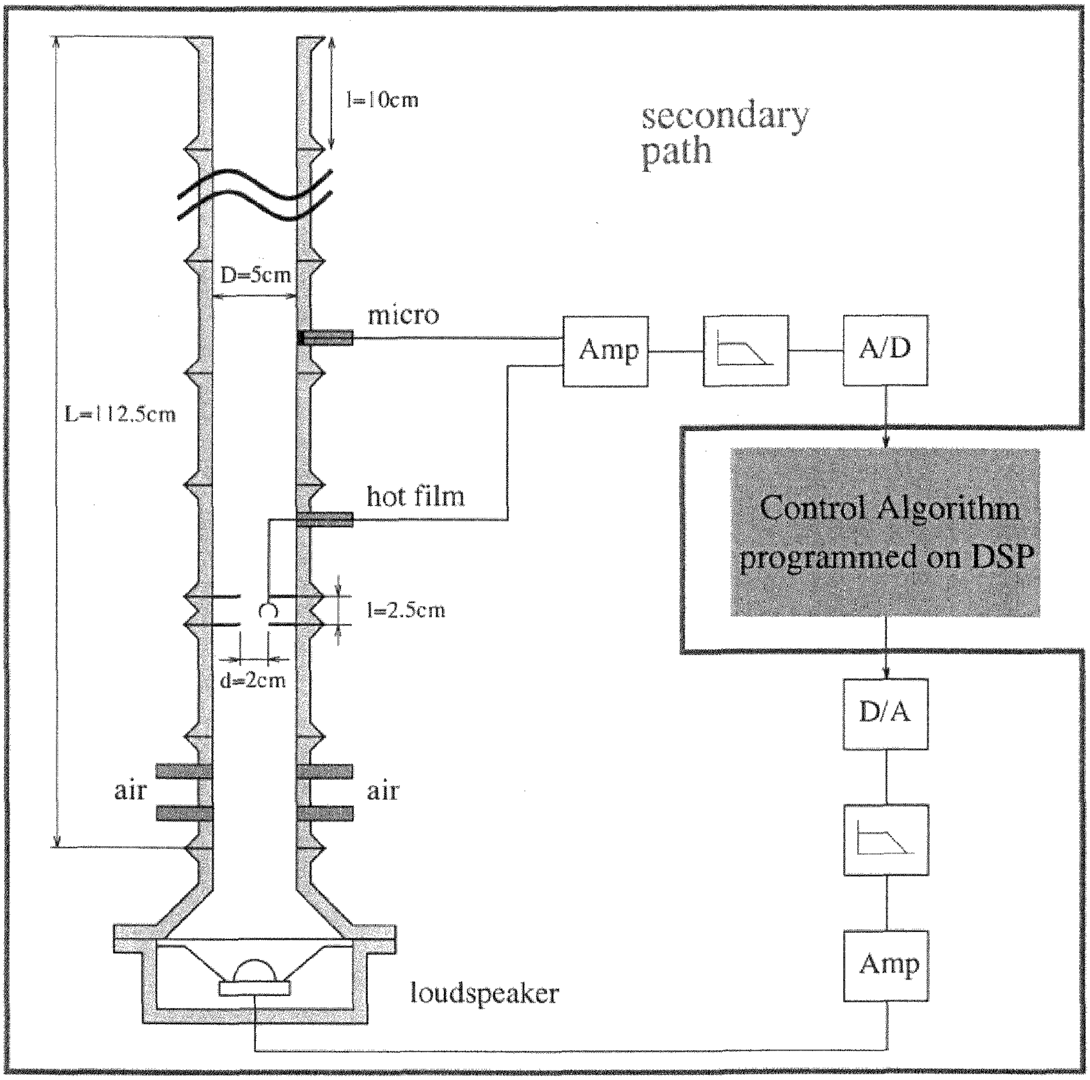

Figure 4: Experimental setup CAPS. The pressure signal is measured by a microphone, the flow velocity by a hot wire. The loudspeaker serves as actuator during control. The secondary path is given by the transfer function between the output of the control algorithm and its own input (inside the thick line).

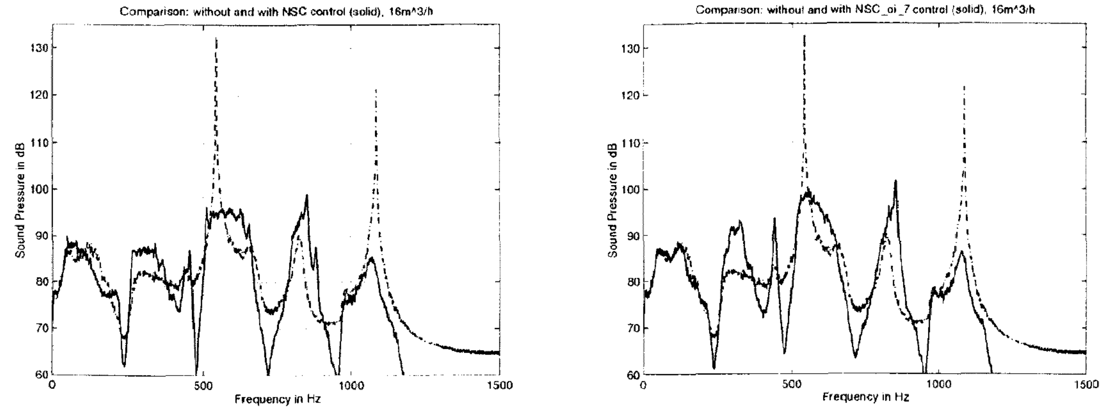

Figure 5: Pressure spectra (----) without and (——) with control. Volume flow rate of 16 m^3/h. On the left: reference algorithm, on the right: SAC scheme.

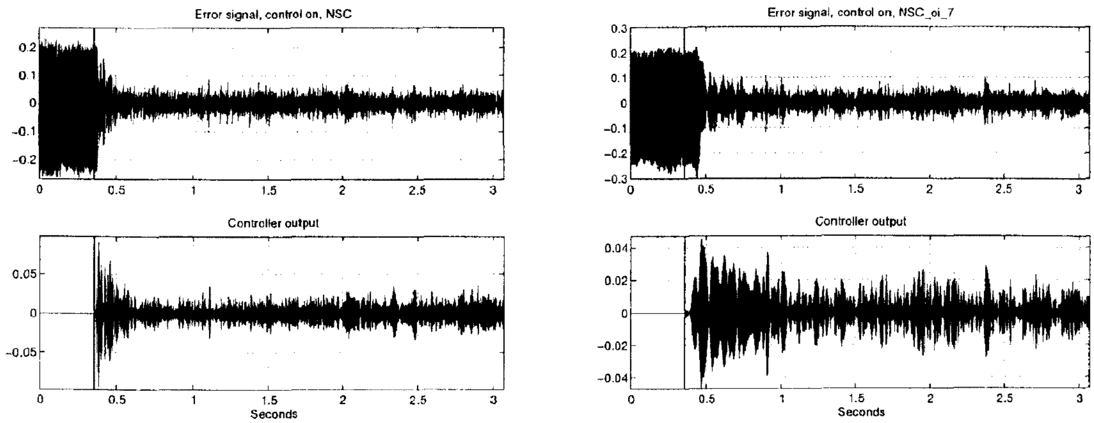

Figure 6: Error sensor (top) and control output (bottom) for a volume flow rate of 16 m^3/h. On the left: reference algorithm, on the right: SAC scheme. Switch on of the control (vertical line).

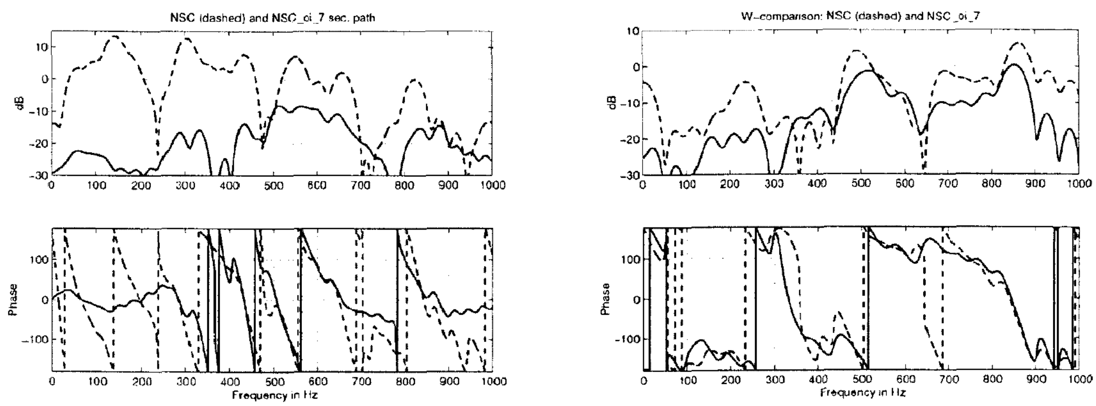

Figure 7: Comparison of the filter tranfer functions. On the left: $\hat{\boldsymbol{S}}$, on the right: $\boldsymbol{W}$ for the reference algorithm (----) and the SAC scheme (——). The amplitudes are on the top figures, the phases on the bottom.

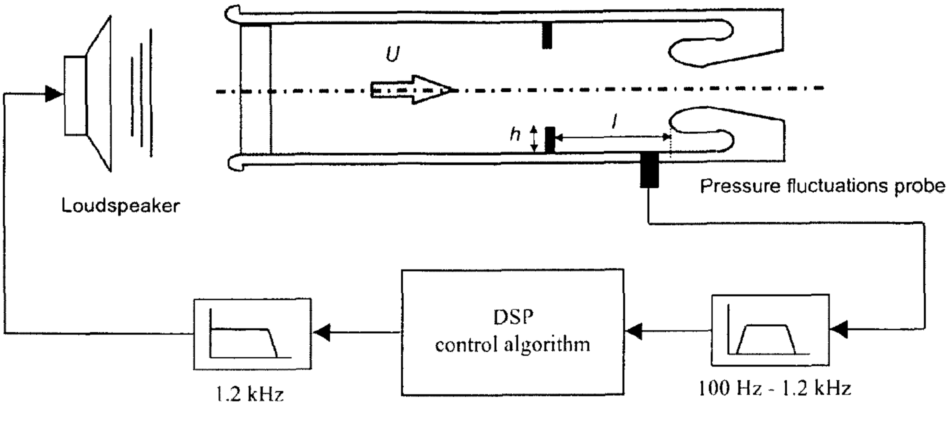

Figure 8: Sketch of the PLEXI facility and the control system.

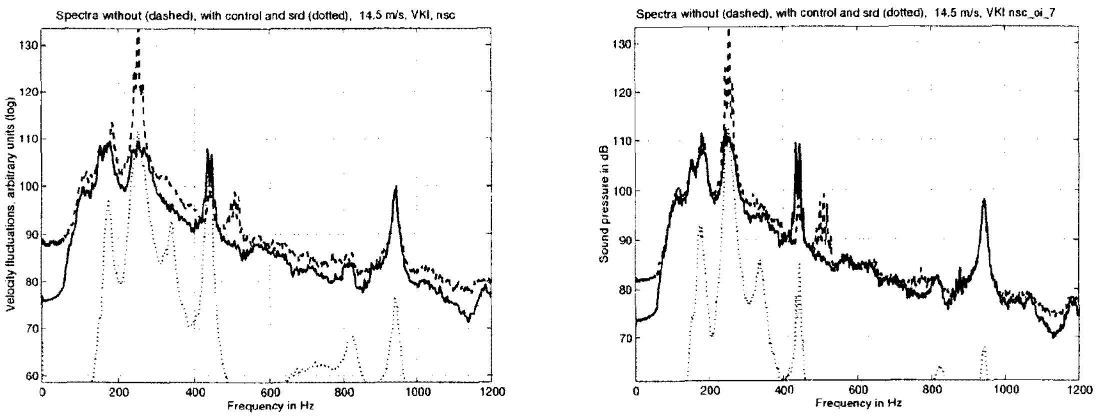

Figure 9: Pressure spectra without (----) and with (——) control. The flow speed is 14.5 m/s. On the left: the reference algorithm, on the right: the SAC scheme.

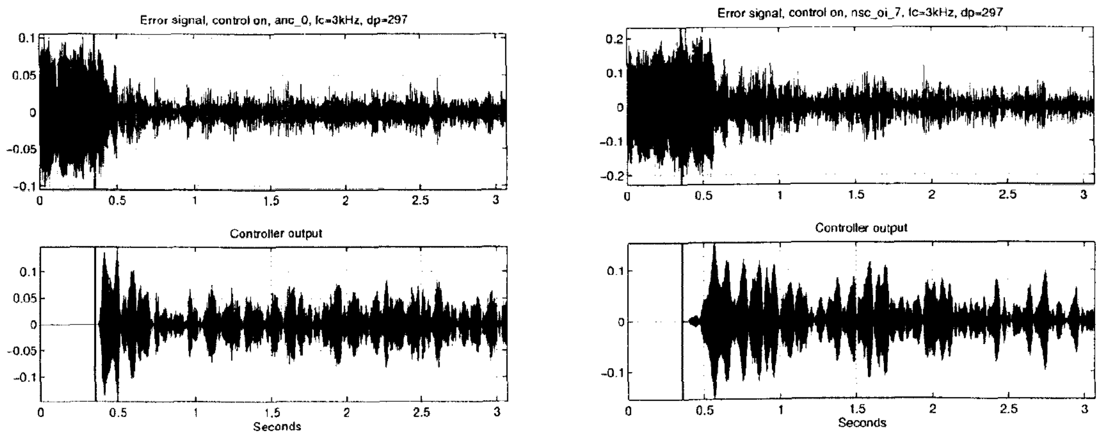

Figure 10: Error signal (top) and controller output (bottom) for a flow speed of 14.5 m/s. On the left: the reference algorithm, on the right: the SAC scheme. Vertical line: switch on of the controller.

PAPER -26, M. Mettenleiter

Question (A. Annaswamy, USA)

Regarding divergence of the coefficients of S: is adding a "leak" term sufficient? Do you understand enough about the "leak" so that you know when to add the "leak" terms?

Reply

The leak is a standard technique in adaptive controllers. We have devised a special technique to tune this procedure (see the paper for more information)

Question (S. Evesque, UK)

Did you try to vary the self-excited mode in the experiment while active control with in-line system identification was applied and, if yes, how well did the controller perform? Same question with off-line system identification. Also, how do you compare performance of FIR and IIR filters in your experiments?

Reply

Varying the self-excited mode was already tested in our initial work on adaptive control of the instability (Billard *et al.*, 1992). It has been tested with the present controller for off-line identification and it works because in this case the secondary path does not change too much. It also works well with the online system. If the secondary path changes, the online algorithm performs better.

Regarding FIR versus IIR filters, it was possible to represent the necessary impulse responses with an FIR filter without too many coefficients. There is no improvement with an IIR system.

Question (F. E. C. Culick, USA)

Do you have any results for flow visualization to show what's happening? What do you think is the origin (mechanisms) of the transfer of energy from vortices to the acoustic pressure field?

Reply

We have carried out experiments at the VKI in which adaptive control was used to suppress oscillations in a configuration simulating the back end of a rocket motor. In these experiments, the flow field was characterized with PIV and the vortices were detected. A statistical analysis of these structures (with and without oscillation) was carried out and this is reported in an article submitted to JFM.

The origin of the transfer of energy is probably (based on experiments at VKI), the periodic impingement of the vortices on the downstream obstacle or nozzle lips.

This page has been deliberately left blank

Page intentionnellement blanche